Hydrogen Addition Strategy for Lean Limit Extension of a Natural Gas Engine

C. Bleechmore, S. Brewster, H. Hochstadt
Orbital Corporation Ltd.

ABSTRACT

The current study evaluates CNG and a hydrogen/methane mixture directly injected into the cylinder of a spark ignition engine. The effects of hydrogen addition with this strategy are compared to operation on pure CNG in terms of engine emissions, thermal efficiency and combustion behaviour including stability at the lean limit of operation.

INTRODUCTION

Gaseous fuels are witnessing strong growth in terms of product in the market and infrastructure. Dominant in this area are engines fuelled by compressed or liquefied natural gas, which now have an established position in the medium and heavy duty sector. Such gaseous fuelled engines may offer an advantage with regard to particulate emissions and CO_2 at point of use, and further developments using higher rates of cooled EGR or lean operation may improve efficiency and reduce aftertreatment requirements, but advantages are constrained by the dilute combustion limits of methane.

Hydrogen is proposed as a gaseous alternative to fossil fuel, and the unique combustion characteristics of hydrogen make it well suited for operation in internal combustion engines. The wide flammability limits, high flame speed and low quenching gap of hydrogen permits very lean operation and in turn, high thermal efficiency with near zero emissions [1]. However the lack of hydrogen infrastructure prevents the wide-scale introduction of purely hydrogen fuelled vehicles. One practical route to reduce dependence on non-renewable gaseous fuels is the blending of hydrogen with CNG which enables the use of existing infrastructure. The combustion of hydrogen and CNG blends in internal combustion engines is therefore an area of particular interest.

Previous work on blends of hydrogen with gaseous and liquid fuels has shown extension of lean limit, improvements in thermal efficiency and reductions in emissions [2-4]. Direct injection of gaseous fuels has proven to extend the load range of engines when naturally aspirated [5,6], and on boosted engines may offer similar advantage to that for liquid fuels [7]. This study aims to build on previous work investigating the direct injection of hydrogen [1] and CNG [5] by evaluation of an HCNG blend. It is thereby intended to aid understanding of HCNG as an alternative fuel, and further develop a direct injection methodology enabling the optimum use of numerous fuels within a single engine architecture. The “one engine | any fuel” philosophy of FlexDI™ Direct Injection is considered significant in addressing the challenge of transport fuel diversification [8].

TEST SETUP

ENGINE TEST BED

Test work has been carried out with a 4-stroke single cylinder research engine. The engine has a centrally located direct injector and close proximity spark plug (Figure 1). In-cylinder pressure was measured using a water-cooled piezoelectric type pressure transducer (KISTLER 6061). The engine specifications are detailed in Table 1.

Engine	Single cylinder
Displacement	454 cc
Bore	82 mm
Stroke	86 mm
Number of valves	4
Compression ratio	12.4:1
Engine speed	2000 RPM
Piston	High compression with bowl
EVO	133 °$aTDC_f$ (587 °$bTDC_f$)
EVC	357 °$aTDC_f$ (363 °$bTDC_f$)
IVO	364 °$aTDC_f$ (356 °$bTDC_f$)
IVC	583 °$aTDC_f$ (137 °$bTDC_f$)

Table 1 Engine specification.

FUEL INJECTOR

A gaseous direct injector (Figure 2) was used for the duration of the testing. This prototype injector was originally developed for boosted CNG engines of 450cc capacity per cylinder [5].

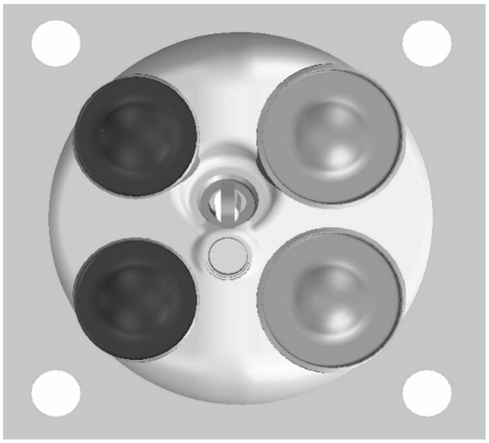

Figure 1 Four valve head with centrally located injector and spark plug.

Figure 2 Gas direct injector.

FUEL PROPERTIES

The fuels tested in this study are compressed natural gas (CNG) and a mixture of hydrogen, methane and nitrogen to represent HCNG. The properties of methane, HCNG and hydrogen are summarised in Table 2. The detailed composition of the test fuels is included in the appendix.

	CH_4	HCNG	H_2
Density (kg/m^3)*	0.717	0.800	0.090
Specific volume (m^3/kg)*	1.39	1.25	11.12
Specific gravity (air =1)*	0.555	0.619	0.0695
Lower heating value (MJ/kg)	50.0	42.7	120.0
Lower heating value (MJ/m^3)*	35.9	34.2	10.8
Higher heating value (MJ/kg)	55.3	47.5	141.9
Higher heating value (MJ/m^3)*	39.8	59.3	12.7
Stoichiometric AFR	17.16	14.33	34.14
LHV of stoichiometric mixture (MJ/kg)	2.75	2.79	3.41
LHV of stoichiometric mixture (MJ/m^3)*	2.12	2.16	2.17
Wobbe Index	53.4	75.4	48.3
CO_2 produced (g/g fuel)	2.74	2.03	0.00
CO_2 produced per energy content (g/kJ)	0.055	0.048	0.000
Limits of flammability in air (vol. %)	5 - 15	-	4 - 77
Laminar burning velocity in air (m/s)	0.37 - 0.43	-	2 - 2.3
Quenching gap in air (mm)	2.03	-	0.64
Diffusion coefficient (cm^2/s)	0.16	-	0.61

Table 2 Fuel properties. (* 0°C, 101.3 kPa)

TEST PROCEDURE

The testing was conducted at 2000 RPM and at two load points; 300 kPa IMEP and wide open throttle. Initially, sweeps of ignition timing and air fuel ratio were completed at part load with CNG to establish a baseline for thermal efficiency, pollutant formation and combustion stability. This set of experiments was then repeated using the HCNG mixture. Scans of injection timing and ignition timing where completed at wide open throttle and stoichiometric air fuel ratio to compare power output, volumetric efficiency, thermal efficiency and pollutant formation of the two fuels.

RESULTS AND DISCUSSION

PART LOAD AIR FUEL RATIO

Tests were conducted at 300 kPa IMEP to determine the effects of air fuel ratio on thermal efficiency, pollutant formation, and combustion stability for the two fuels. Two injection timings were tested; start of injection at 240° bTDC (before intake valve closure) and 120° bTDC (after intake valve closure). Lambda was varied from 1.0 to the lean limit in 0.1 increments. For each injection timing and air fuel ratio, ignition timing was optimised for indicated thermal efficiency.

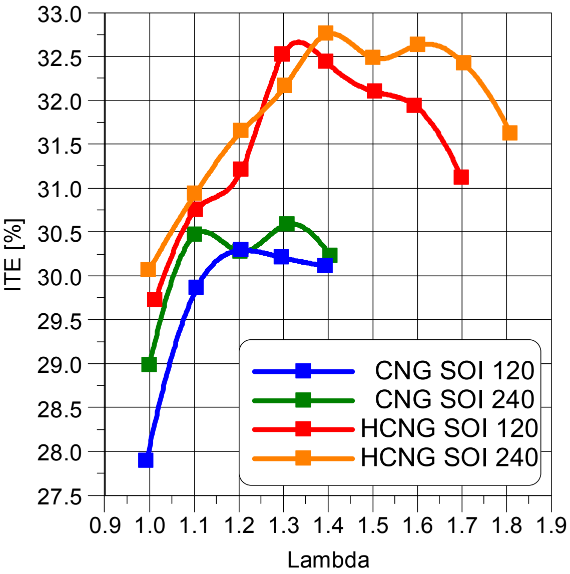

Figure 3 Indicated thermal efficiency at 300 kPa IMEP.

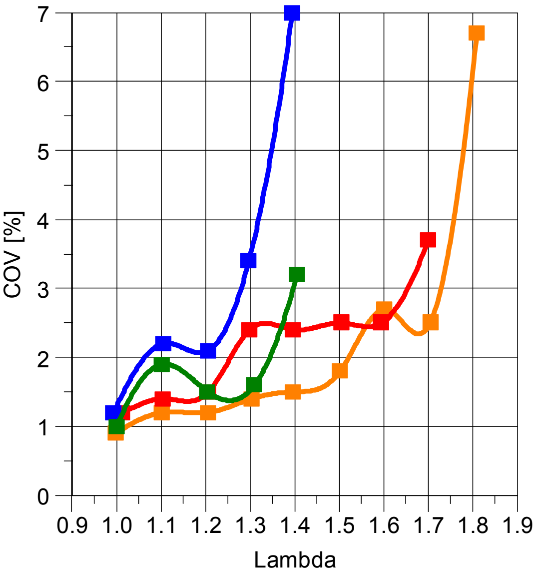

Figure 4 Combustion stability at 300 kPa IMEP.

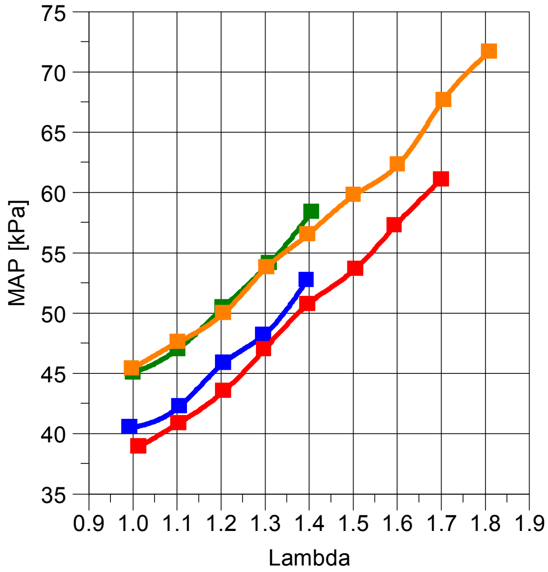

Figure 5 Manifold air pressure at 300 kPa IMEP.

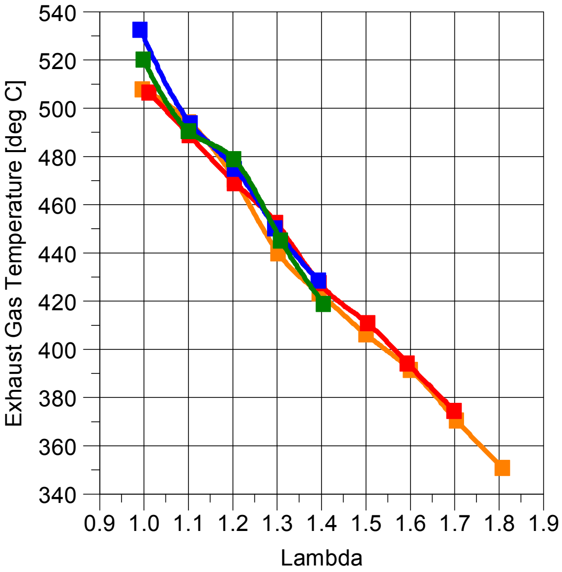

Figure 6 Exhaust gas temperature at 300 kPa IMEP.

For both fuel types, indicated thermal efficiency (Figure 3) increases as lambda increases. The HCNG blend yields higher efficiency especially at leaner air fuel ratios. Fuel injected at the earlier timing returned higher efficiency due to improved mixture preparation and reduced pumping work resulting from higher intake manifold pressure (Figure 5). The addition of hydrogen improves combustion stability (Figure 4) and extends the lean limit to lambda 1.8. The lean limit extension further reduces exhaust gas temperature (Figure 6).

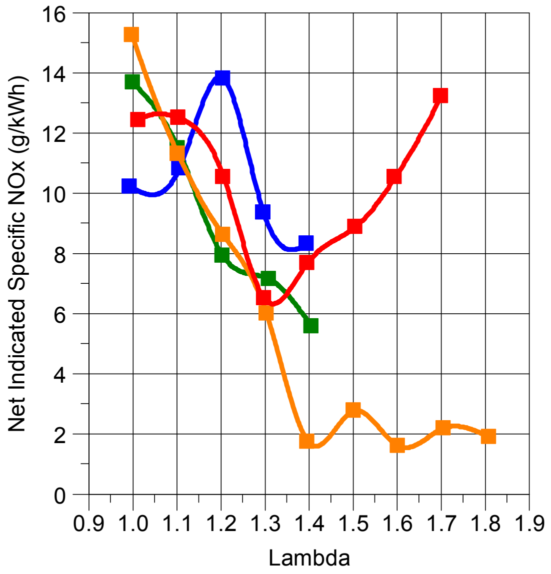

Figure 7 Net indicated specific NO_x emission at 300 kPa IMEP.

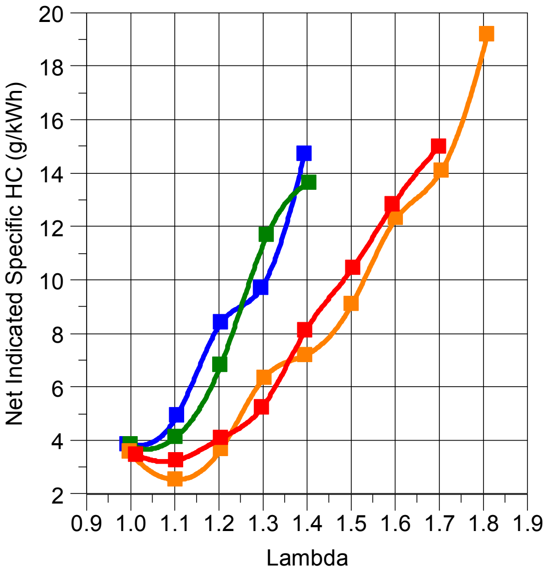

Figure 8 Net indicated specific HC emission at 300 kPa IMEP.

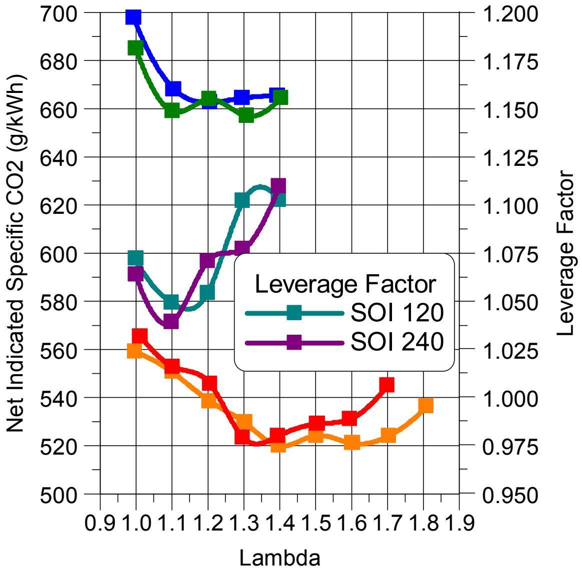

Figure 9 Net indicated specific CO2 emission at 300 kPa IMEP.

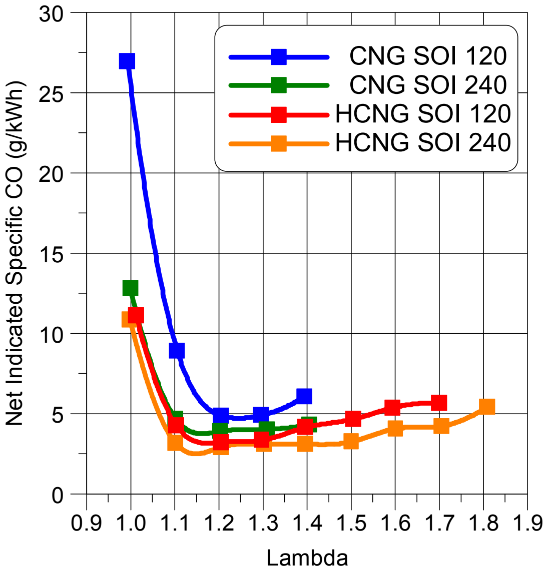

Figure 10 Net indicated specific CO emission at 300 kPa IMEP.

The two fuels produce similar amounts of NO_x (Figure 7) at lambda 1.1 and 1.2. At air fuel ratios leaner than lambda 1.4, HCNG injected at the early timing produces in the order of 2 g/kWh of NO_x. This trend is not observed for the late injection timing due to higher peak gas temperatures. Hydrocarbons (Figure 8) in the exhaust gas with HCNG are approximately half that of CNG when operating leaner than lambda 1.1. They are similar at stoichiometric conditions and injection timing has minimal effect. Production of carbon dioxide (Figure 9) is lower for the HCNG mixture mainly due to displacement by hydrogen but also higher thermal efficiency. This effect can be quantified using a “leverage factor” which normalises the reduction in CO_2 emission from using HCNG against the reduction in carbon content of the fuel, and which has a value consistently greater than unity.

$$\text{Leverage Factor} = \frac{\text{Actual Improvement}}{\text{Theoretical Improvement}}$$

$$\text{Leverage Factor} = \frac{CO_{2CNG}[g/kWh]}{CO_{2HCNG}[g/kWh]} \div \frac{CO_{2CNG}[g/kJ]}{CO_{2HCNG}[g/kJ]}$$

Trends in carbon monoxide (Figure 10) production are similar for the four data sets, except for HCNG causing less CO formation at the stoichiometric condition. The earlier injection timing returns lower CO emission due to improved mixing prior to combustion.

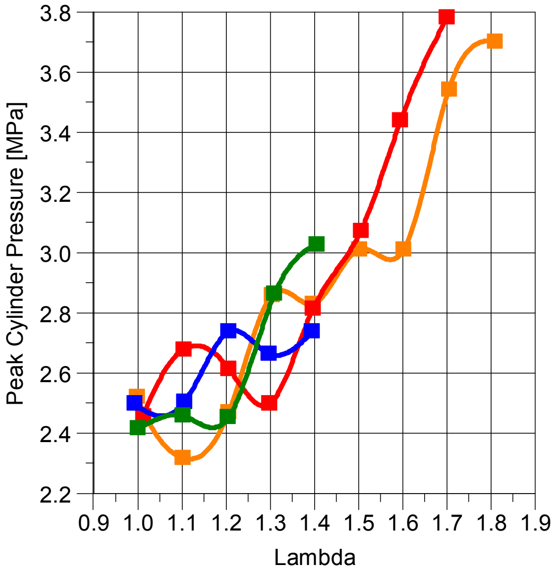

Figure 11 Peak cylinder pressure at 300 kPa IMEP.

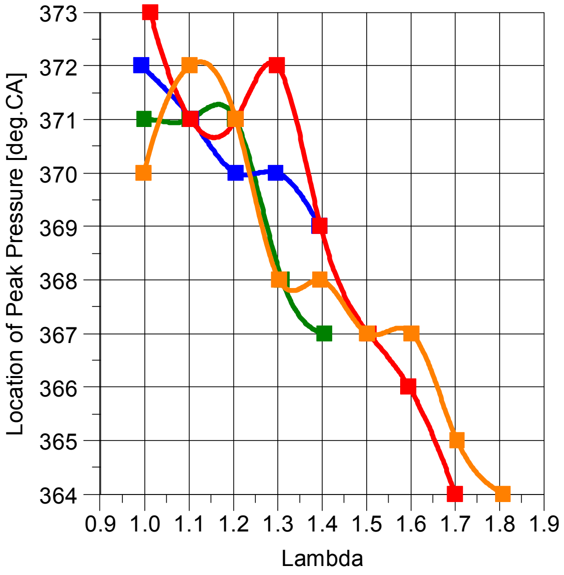

Figure 12 Location of peak pressure at 300 kPa IMEP.

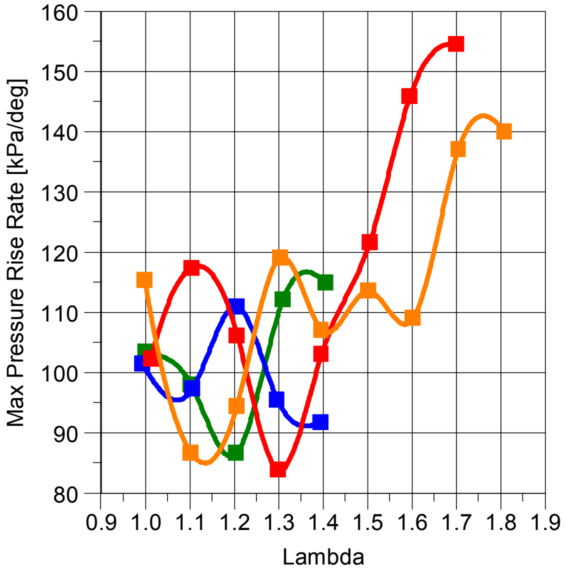

Figure 13 Maximum pressure rise rate at 300 kPa IMEP.

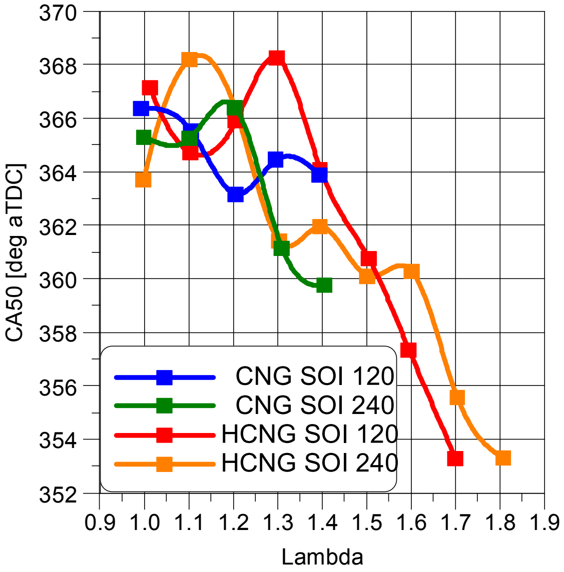

Figure 14 Location of 50% mass fraction burn at 300 kPa IMEP.

Peak cylinder pressure (Figure 11) is similar for the four cases tested and the general trend is increasing as lambda increases. The location of peak pressure (Figure 12) advances as lambda increases independent of fuel type and injection timing. The maximum pressure rise rate (Figure 13) increases rapidly for HCNG at lambda greater than 1.4. This can be explained by the earlier optimum phasing of the combustion event.

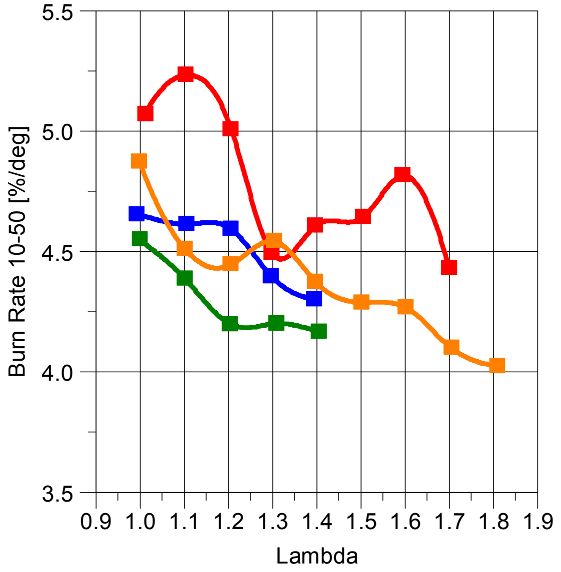

Figure 15 Burn rate at 300 kPa IMEP.

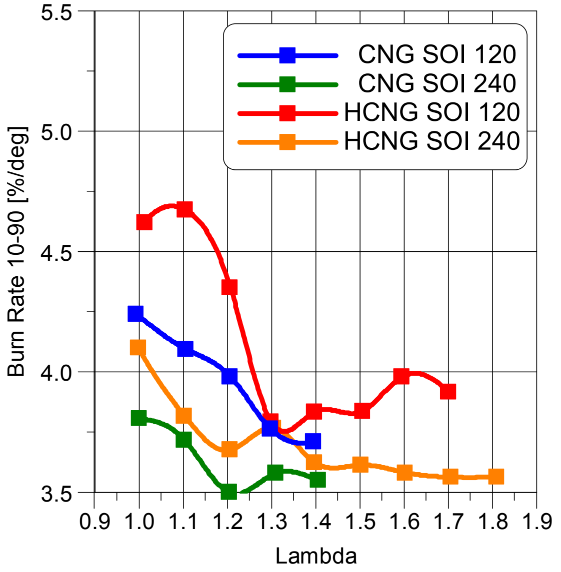

Figure 16 Burn rate at 300 kPa IMEP.

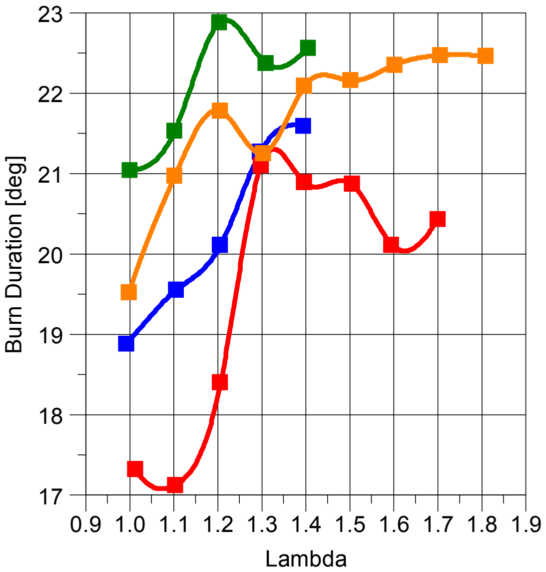

Figure 17 Burn duration at 300 kPa IMEP.

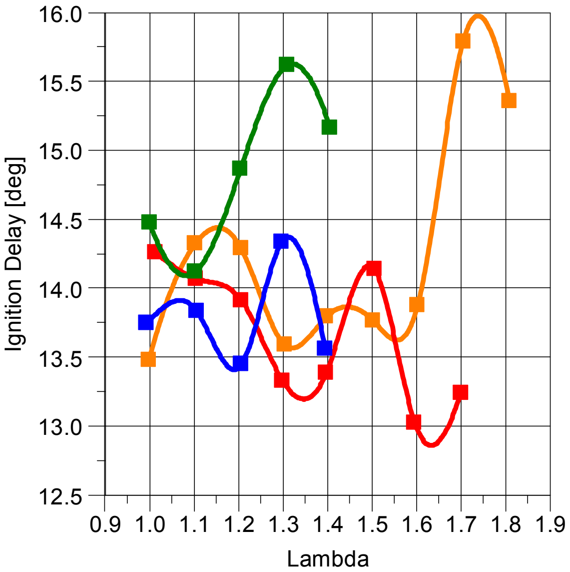

Figure 18 Ignition delay at 300 kPa IMEP.

The observed burn rates (Figure 15, Figure 16) generally decrease as the mixture becomes leaner. Burn rates for the late fuel injection timing setting are faster, suggesting some level of stratification is occurring. HCNG combustion occurred more rapidly than CNG at the same injection timing. Ignition delay (Figure 18) is similar for the four cases until the lean limit of each fuel is reached. At the lean limit, where fuel was injected at the earlier timing, ignition delay increases sharply. This is not observed when the fuel is injected later, further suggesting some level of stratification of the fuel near the spark plug is occurring.

FULL LOAD INJECTION SCAN

Tests were completed at 2000 RPM with wide open throttle and stoichiometric air fuel ratio. The injecting timing was varied from 120° to 360° bTDC and wide open throttle performance, pollutant formation and combustion metrics were compared.

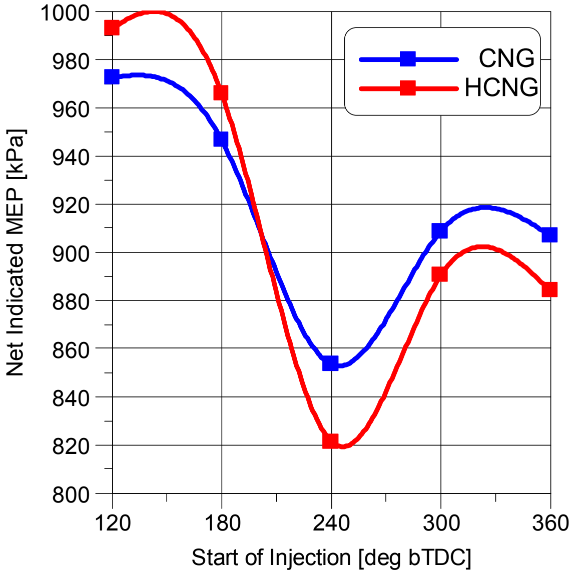

Figure 19 Net indicated mean effective pressure at wide open throttle.

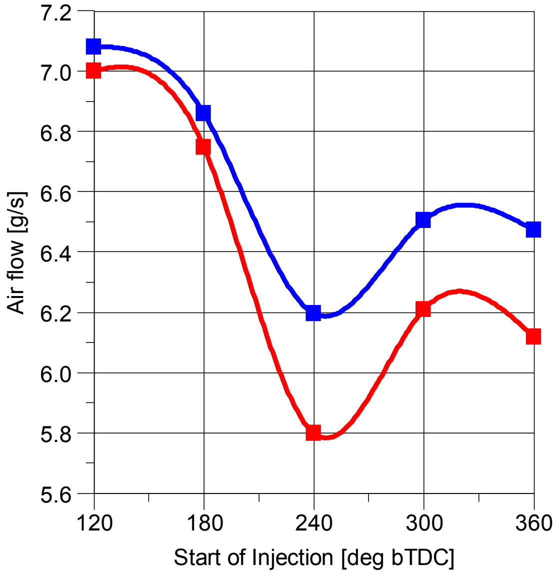

Figure 20 Airflow at wide open throttle.

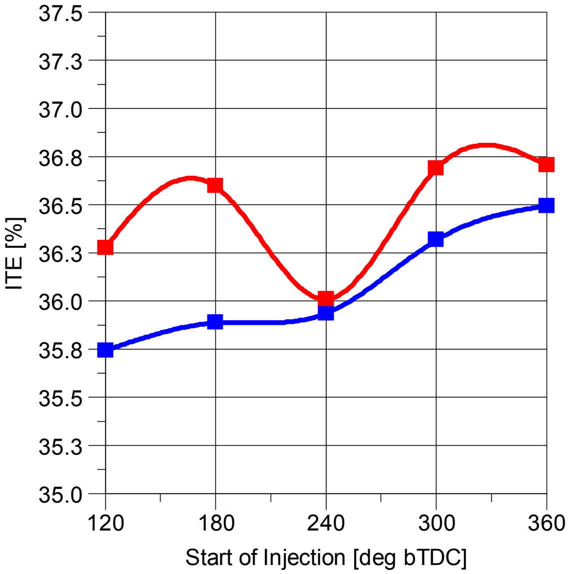

Figure 21 Indicated thermal efficiency at wide open throttle.

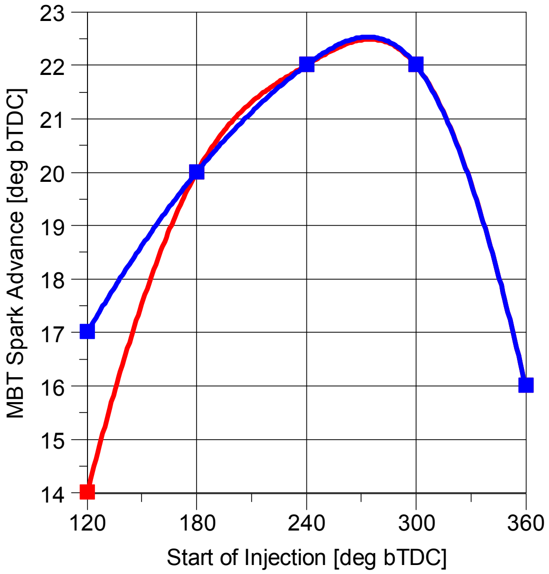

Figure 22 MBT ignition timing at wide open throttle.

When injection occurs either fully or partially after intake valve closure, higher IMEP (Figure 19) and airflow (Figure 20) are achieved. Under these conditions, HCNG performs better than CNG. For earlier injection timings displacement of air by fuel is greater with HCNG and lower IMEP results. Airflow and IMEP is lowest with injection timing at 240° bTDC. Indicated thermal efficiency (Figure 21) is slightly higher for HCNG. The spark advance producing maximum torque (Figure 22) for the two fuels are identical for all injection timings except 120° bTDC.

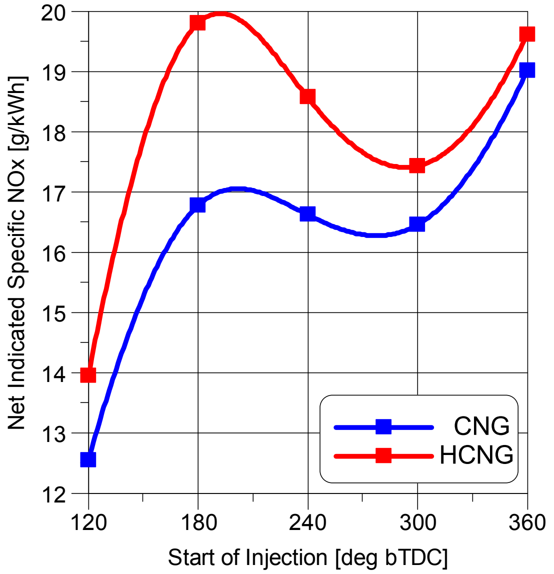

Figure 23 Net indicated specific NOx emission at wide open throttle.

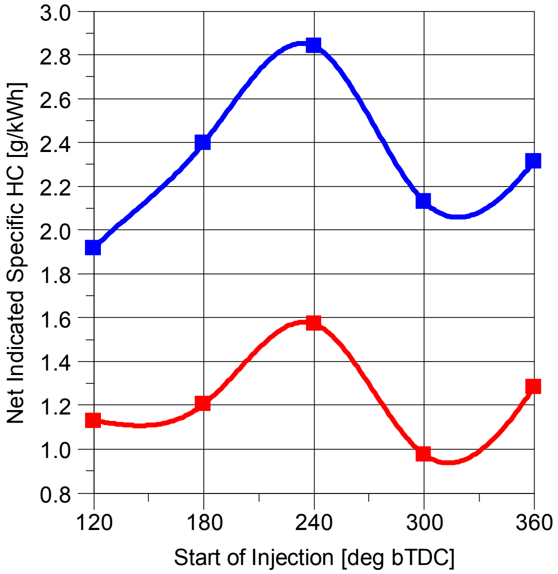

Figure 24 Net indicated specific HC emission at wide open throttle.

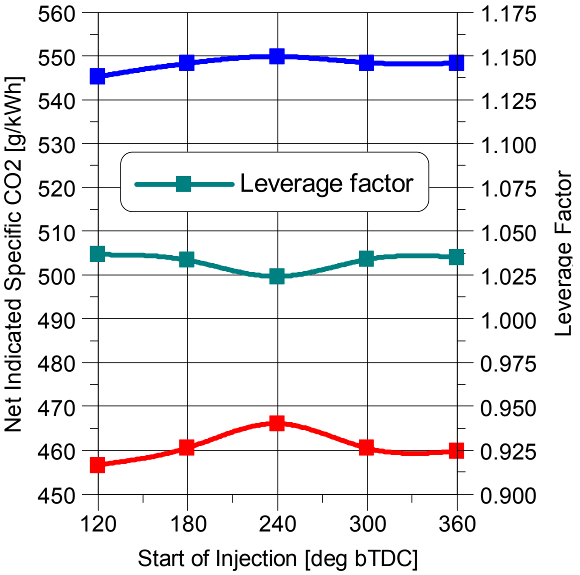

Figure 25 Net indicated specific CO_2 emission at wide open throttle.

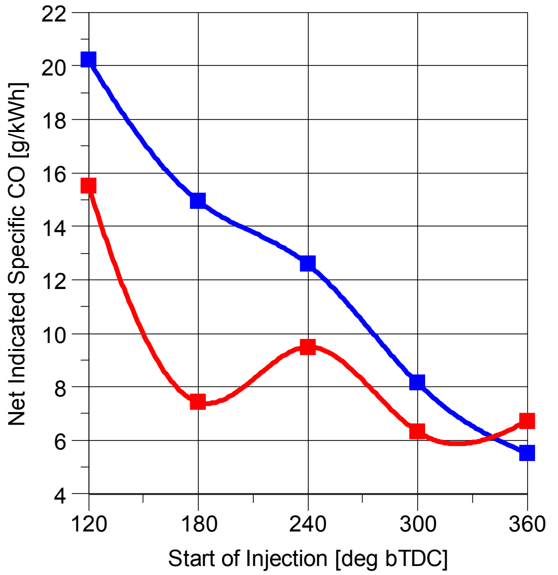

Figure 26 Net indicated specific CO emission at wide open throttle.

Operation on HCNG produces more NO_x than CNG at all injection timings (Figure 23) due to higher peak combustion temperatures. Hydrocarbon emissions (Figure 24) are less for HCNG suggesting that the hydrogen promotes a more complete burn. Formation of CO_2 (Figure 25) is significantly reduced with HCNG compared to CNG mostly due to the lower carbon content of the fuel, but also in part due to higher thermal efficiency. The "leverage factor" does not vary significantly with injection timing. Increased levels of carbon monoxide (Figure 26) at later injection timings can be attributed to less time for mixing of the fuel and air, resulting in localised rich combustion. Carbon monoxide production is lower for HCNG.

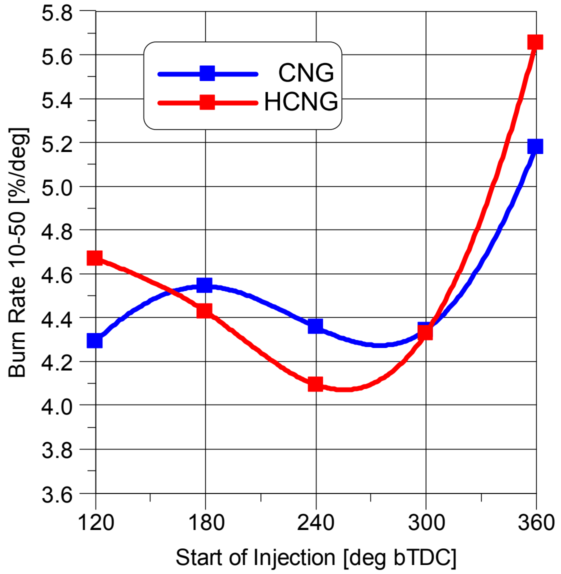

Figure 27 Burn rate at wide open throttle.

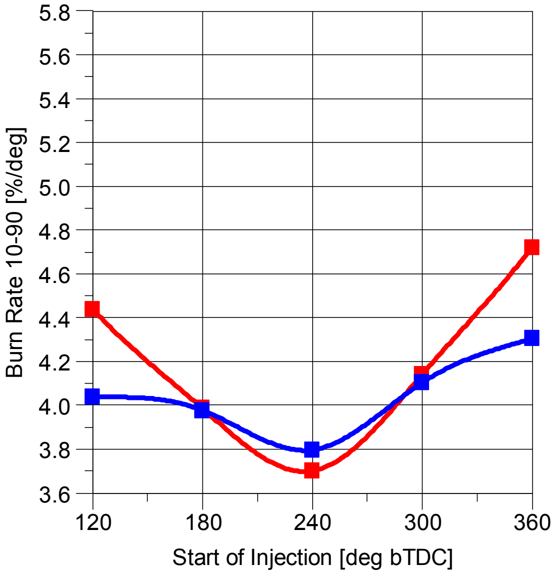

Figure 28 Burn rate at wide open throttle.

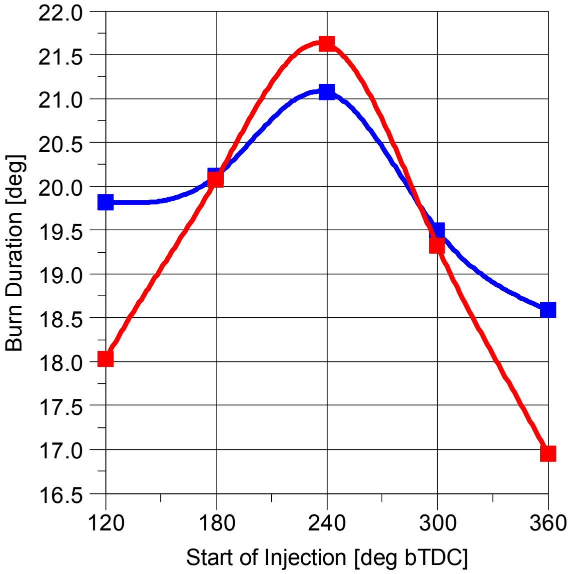

Figure 29 Burn duration at wide open throttle.

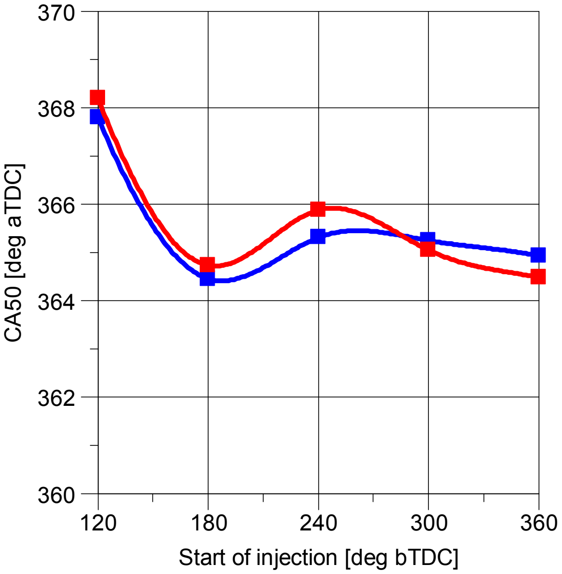

Figure 30 Location of 50% mass fraction burn at wide open throttle.

The initial burn rate (Figure 27) of the two fuels is significantly higher at the earliest start of injection timing compared with the later injection timings. The increased time allowed for mixing increases the initial and total burn rate (Figure 28). Burn duration (Figure 29) is dependent on trapped charge density and mixture preparation. As a result, the 240° bTDC injection timing is the slowest burning case for both fuels. HCNG is observed to be more sensitive to injection timing due to its higher specific volume.

CONCLUSION

At the part load condition, earlier direct injection timing returned higher efficiency and lower emissions for both fuels. At part load the HCNG mixture:

- extends the lean operating limit to lambda 1.8 from 1.4 for CNG alone,
- increases maximum indicated thermal efficiency from 30.6% to 32.8%.
- lowers exhaust temperatures by extension of lean limit.
- returns NO_x formation of 2 g/kWh when operating leaner than lambda 1.4 with HCNG
- reduces hydrocarbon emissions by 40% and
- reduces CO_2 emissions by 21%.

At the full load condition, the use of HCNG increases the engine output when injecting the fuel after intake valve closure. For earlier injection timings however, more air is displaced by HCNG resulting in lower output. At the full load condition:

- indicated thermal efficiency is higher for HCNG at all injection timings,
- formation of NO_x is higher for HCNG at all the injection timings tested,
- hydrocarbon emissions are reduced by approximately 40%, and
- CO_2 emissions are reduced by 16% with HCNG.

Addition of hydrogen to methane in ratio of 30% by volume and in stoichiometric operation may be understood to offer a slight increase in engine thermal efficiency coupled with significant reductions in emissions of CO_2 and HC, although with a slight increase in NOx. Further, the addition of hydrogen enables a significant extension of the lean limit, providing further increases in efficiency, reductions in CO_2, NOx and HC, and reduction in exhaust gas temperature. It may be proposed that the addition of hydrogen to CNG in a lean limit extension strategy would allow higher engine operating efficiency coupled with reduced demand on NOx aftertreatment, and reduced engine thermal loading.

ACKNOWLEDGEMENTS

The authors would like to thank the facilities staff and in particular Doug Barrett for their assistance throughout this project.

REFERENCES

1. Bleechmore C., Brewster S. “Dilution Strategies for Load and NOx Management in an Hydrogen Fuelled Direct Injection Engine.” SAE paper number 2007-01-4097, 2007
2. Li H., Karim G., “An Experimental Investigation of S.I. Engine Operation on Gaseous Fuels Lean Mixtures.” SAE paper number 2005-01-3765
3. Pede G., Rossi E., Chiesa M., Ortenzi F., “Test of blends of hydrogen and natural gas in a light duty vehicle.” SAE paper 2007-01-2045
4. Das L., Swain R., Polly M., “Performance Improvement of a CNG-Fuelled Spark Ignited Engine by Hydrogen Addition.” SAE paper 2004-28-0033

5. Caley D., Cathcart G., “Development of a Natural Gas Spark Ignited Direct Injection Combustion System.” NGV2006
6. Kim, J., “Development of Direct Injection CNG Engine.” Inha Technical College.
7. Brewster S., “Initial Development of a Turbo-charged Direct Injection E100 Combustion System.” SAE paper 2007-01-3625
8. www.flexdi.com

APPENDIX

CNG specification

Gas	Volume Concentration	Mass Concentration
Nitrogen	2.40%	3.64%
Carbon Dioxide	2.21%	5.27%
Methane	87.30%	75.91%
Ethane	6.16%	10.04%
Propane	1.50%	3.59%
Iso-Butane	0.13%	0.41%
n-Butane	0.20%	0.63%
Neo-Pentane	0.01%	0.02%
Iso-Pentane	0.04%	0.16%
n-Pentane	0.03%	0.12%
Hexanes	0.02%	0.09%
Heptanes	0.01%	0.05%
Octanes	0.01%	0.03%
Nonanes	0.01%	0.03%

HCNG specification

Gas	Volume Concentration	Mass Concentration
Nitrogen	9.80%	21.17%
Hydrogen	30.00%	4.71%
Methane	60.20%	74.12%